*Numerical Algorithms* **30:** 11–23, 2002.


# Computing complex Airy functions by numerical quadrature

Amparo Gil [a,c], Javier Segura [b,c] and Nico M. Temme [d]

[a] *Departamento de Matemáticas, U. Autónoma de Madrid, 28049 Madrid, Spain*
E-mail: amparo.gil@uam.es
[b] *Departamento de Matemáticas, U. Carlos III de Madrid, 28911 Leganés, Madrid, Spain*
E-mail: jsegura@math.uc3m.es
[c] *Universität GhK, FB 17 Mathematik-Informatik, 34132 Kassel, Germany*
[d] *CWI, P.O. Box 94079, 1090 GB Amsterdam, The Netherlands*
E-mail: nicot@cwi.nl

Received 3 August 2001; accepted 20 November 2001
Communicated by S. Paszkowski

Integral representations are considered of solutions of the Airy differential equation $w'' - zw = 0$ for computing Airy functions for complex values of $z$. In a first method contour integral representations of the Airy functions are written as non-oscillating integrals for obtaining stable representations, which are evaluated by the trapezoidal rule. In a second method an integral representation is evaluated by using generalized Gauss–Laguerre quadrature; this approach provides a fast method for computing Airy functions to a predetermined accuracy. Comparisons are made with well-known algorithms of Amos, designed for computing Bessel functions of complex argument. Several discrepancies with Amos' code are detected, and it is pointed out for which regions of the complex plane Amos' code is less accurate than the quadrature algorithms. Hints are given in order to build reliable software for complex Airy functions.

**Keywords:** Airy functions, steepest descent method, saddle point methods numerical computation of special functions, numerical quadrature, Gauss–Laguerre quadrature

**AMS subject classification:** 33C10, 33F05, 41A60, 30E10, 65D20, 65D32

## 1. Introduction

Airy functions are solutions of the differential equation

$$\frac{d^2w}{dz^2} - zw = 0. \tag{1}$$

Two linearly independent solutions that are real for real values of $z$ are denoted by $\mathrm{Ai}(z)$ and $\mathrm{Bi}(z)$. They have the integral representation

$$\begin{aligned} \mathrm{Ai}(z) &= \frac{1}{\pi}\int_0^\infty \cos\left(zt+\frac{1}{3}t^3\right)\mathrm{d}t, \\ \mathrm{Bi}(z) &= \frac{1}{\pi}\int_0^\infty \sin\left(zt+\frac{1}{3}t^3\right)\mathrm{d}t + \frac{1}{\pi}\int_0^\infty \mathrm{e}^{zt-t^3/3}\,\mathrm{d}t, \end{aligned} \tag{2}$$

where we assume that $z$ is real. See [1,10] or [12].

The Airy function has applications in physics (quantum mechanics, scattering problems) and in asymptotics, where it is a main approximant in uniform expansions for solutions of differential equations with turning points, or for integrals with coalescing saddle points.

In this paper we are concerned with the numerical evaluation of $\mathrm{Ai}(z)$ and $\mathrm{Ai}'(z)$ for complex values of $z$ by numerical quadrature. It is convenient to introduce, as in [10], the functions

$$\mathrm{Ai}_0(z) = \mathrm{Ai}(z), \qquad \mathrm{Ai}_1(z) = \mathrm{Ai}\left(\mathrm{e}^{-2\pi\mathrm{i}/3}z\right), \qquad \mathrm{Ai}_{-1}(z) = \mathrm{Ai}\left(\mathrm{e}^{2\pi\mathrm{i}/3}z\right). \tag{3}$$

We have the representations

$$\mathrm{Ai}_j(z) = \frac{\mathrm{e}^{2j\pi\mathrm{i}/3}}{2\pi\mathrm{i}}\int_{\mathcal{C}_{-j}} \mathrm{e}^{-zt+t^3/3}\,\mathrm{d}t, \quad j = 0, \pm 1, \tag{4}$$

where the contours $\mathcal{C}_j$ are given in figure 1. As a consequence, because

$$\int_{\mathcal{C}_0\cup\mathcal{C}_1\cup\mathcal{C}_{-1}} \mathrm{e}^{-zt+t^3/3}\,\mathrm{d}t = 0,$$

we have the following linear combination of three solutions of (1):

$$\mathrm{Ai}(z) + \mathrm{e}^{-2\pi\mathrm{i}/3}\mathrm{Ai}_1(z) + \mathrm{e}^{2\pi\mathrm{i}/3}\mathrm{Ai}_{-1}(z) = 0. \tag{5}$$

The first integral in (2) follows from deforming the contour $\mathcal{C}_0$ in (4) into the imaginary axis. The function $\mathrm{Bi}(z)$ can be written as

$$\mathrm{Bi}(z) = \mathrm{e}^{\pi\mathrm{i}/6}\mathrm{Ai}_{-1}(z) + \mathrm{e}^{-\pi\mathrm{i}/6}\mathrm{Ai}_1(z), \tag{6}$$

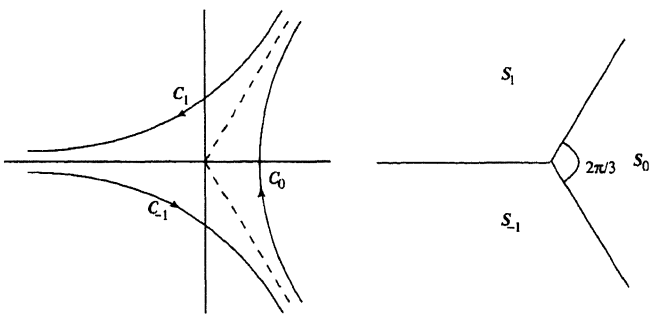


Figure 1. Three contours of integration $\mathcal{C}_j$ for the Airy integrals in (4), and sectors $S_j$ where $\mathrm{Ai}_j(z)$ are recessive.

and the second representation in (2) follows by deforming contour $\mathcal{C}_1$ into the positive imaginary axis and $(-\infty, 0]$, and the contour $\mathcal{C}_{-1}$ into $(-\infty, 0]$ and the negative imaginary axis. We also have

$$\mathrm{Bi}(z) = \mp \mathrm{i}\mathrm{Ai}(z) + 2\mathrm{e}^{\pm\pi\mathrm{i}/6}\mathrm{Ai}_{\mp 1}(z). \tag{7}$$

The function $\mathrm{Ai}_j(z)$ is recessive at infinity in the sector $S_j$, $j = 0, \pm 1$, the function being exponentially small at infinity along the diagonal of this sector. On the other hand, $\mathrm{Ai}_j(z)$ is dominant at infinity in the sectors $S_{j-1}$ and $S_{j+1}$ (the suffix $j$ is enumerated modulo 3), and is exponentially large at infinity along the diagonals of these sectors. $\mathrm{Bi}(z)$ is dominant at infinity within all three sectors $S_j$. A pair of Airy functions comprises a numerically satisfactory pair at infinity within a sector if only one function is dominant. For example, the pair $\{\mathrm{Ai}(z), \mathrm{Bi}(z)\}$ comprises such a pair only in $S_0$ (and on the negative real axis, where none of the two is dominant, but where the phases in their oscillations differ by $\pi/2$).

### *1.1. Existing algorithms*

For an overview of software for the Airy functions we refer to [8]. See also the Guide to Available Mathematical Software at the web site `http://math.nist.gov/gams/`. The main contributions are [2] (where the Airy functions follow from algorithms for the Bessel functions) and [11], where integral representations of Stieltjes type and generalized Gauss quadrature with tabulated weights and abscissae were used. In [3] Taylor series and asymptotic expansions are used; in a second method, a grid of points in the complex plane is used where the functions are known to high precision, and Taylor series are then used from these base points.

Interactive systems like Maple and Mathematica also include algorithms for complex Airy functions.

## 2. Principal domain for computation

For the numerical evaluation of $\mathrm{Ai}(z)$ we concentrate on the principal sector

$$\mathcal{S} = \left\{ z \mid \mathrm{ph}z \in \left[ -\frac{2\pi}{3}, \frac{2\pi}{3} \right] \right\}. \tag{8}$$

When $\Im z < 0$ we use complex conjugation, because of

$$\mathrm{Ai}(x - \mathrm{i}y) = \overline{\mathrm{Ai}(x + \mathrm{i}y)}.$$

If

$$\mathrm{ph}z \in \left( \frac{2\pi}{3}, \pi \right] \quad \text{or} \quad \mathrm{ph}z \in \left( -\pi, -\frac{2\pi}{3} \right),$$

that is, $z \notin \mathcal{S}$, $z\mathrm{e}^{\pm 2\pi\mathrm{i}/3}$ are both inside $\mathcal{S}$, and we can use (see (5))

$$\mathrm{Ai}(z) = -\mathrm{e}^{-2\pi\mathrm{i}/3}\mathrm{Ai}\left(\mathrm{e}^{-2\pi\mathrm{i}/3}z\right) - \mathrm{e}^{2\pi\mathrm{i}/3}\mathrm{Ai}\left(\mathrm{e}^{2\pi\mathrm{i}/3}z\right). \tag{9}$$

At most one of the Airy functions at the right-hand side is dominant if $z \notin \mathcal{S}$.

## 3. Steepest descent contours

For details on the saddle point method and steepest descent contours we refer to [10] or [13].

We consider

$$\mathrm{Ai}(z) = \int_{\mathcal{C}_0} \mathrm{e}^{w^3/3 - zw}\, \mathrm{d}w, \tag{10}$$

where $\mathrm{ph} z \in [0, 2\pi/3]$ and $\mathcal{C}_0$ is the contour shown in figure 1. Let

$$\phi(w) = \frac{1}{3}w^3 - zw. \tag{11}$$

The saddle points are $w_0 = \sqrt{z}$ and $w = -w_0$ and follow from solving $\phi'(w) = w^2 - z = 0$.

The path of steepest descent through the saddle point $w_0$ is defined by

$$\Im\big[\phi(w)\big] = \Im\big[\phi(w_0)\big]. \tag{12}$$

We write

$$z = x + \mathrm{i}y = r\mathrm{e}^{\mathrm{i}\theta}, \qquad w = u + \mathrm{i}v, \qquad w_0 = u_0 + \mathrm{i}v_0. \tag{13}$$

Then

$$u_0 = \sqrt{r}\cos\frac{\theta}{2}, \qquad v_0 = \sqrt{r}\sin\frac{\theta}{2}, \qquad x = u_0^2 - v_0^2, \qquad y = 2u_0v_0. \tag{14}$$

We have

$$\psi_r(\sigma,\tau) = \Re\big[\phi(w) - \phi(w_0)\big] = u_0\big(\sigma^2 - \tau^2\big) - 2v_0\sigma\tau + \frac{1}{3}\sigma^3 - \sigma\tau^2, \tag{15}$$

$$\psi_i(\sigma,\tau) = \Im\big[\phi(w) - \phi(w_0)\big] = v_0\big(\sigma^2 - \tau^2\big) + 2u_0\sigma\tau - \frac{1}{3}\tau^3 + \sigma^2\tau, \tag{16}$$

where

$$\sigma = u - u_0, \qquad \tau = v - v_0. \tag{17}$$

The path of steepest descent through $w_0$ is given by the equation

$$u = u_0 + \frac{(v - v_0)(v + 2v_0)}{3\big[u_0 + \sqrt{(v^2 + 2v_0v + 3u_0^2)/3}\big]}, \qquad -\infty < v < \infty. \tag{18}$$

Examples for $r = 5$ and a few $\theta$ values are shown in figure 2. The saddle points are located on the circle with radius $\sqrt{r}$ and are indicated by small dots. The saddle point on the positive axis is for the case $\theta = 0$ and the two saddles on the imaginary axis are for $\theta = \pi$. This is out of the range of present interest, but it is instructive to

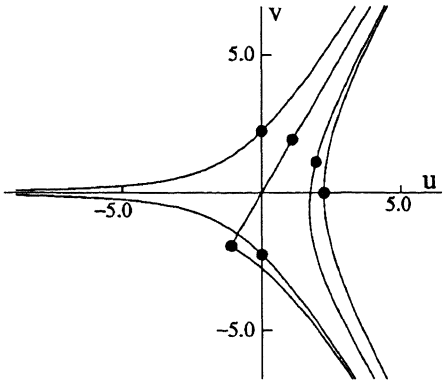


Figure 2. Saddle point contours for $r = 5$ and $\theta = 0, \pi/3, 2\pi/3, \pi$.

see that for $-z \in S_0$ the contour splits up and runs through both saddle points $\pm w_0$. For $\theta = 2\pi/3$ one part of the contour is given by the half line $v = \sqrt{3}u$ and the other part (through $-w_0$) by

$$u = u_0 - \frac{(v - v_0)(v + 2v_0)}{\sqrt{3}v}, \quad v < -v_0. \tag{19}$$

We see that when $z$ crosses the line $\mathrm{ph}z = 2\pi/3$ the saddle point $-w_0$ becomes important. This aspect is connected with the Stokes phenomenon in asymptotics, and the half-line $\mathrm{ph}z = 2\pi/3$ is a Stokes line for $\mathrm{Ai}(z)$, just as the half-lines $\mathrm{ph}z = -2\pi/3$ and $\mathrm{ph}z = 0$. Observe that the values of $\exp(\Re\phi(w))$ (see (11)) at $w = \pm w_0$, which are dominant terms in the asymptotic representations of the Airy functions, are given by

$$\exp\left(-\frac{2}{3}r^{3/2}\cos\frac{3\theta}{2}\right), \qquad \exp\left(\frac{2}{3}r^{3/2}\cos\frac{3\theta}{2}\right),$$

respectively, and one of these dominates the other one optimally at the Stokes lines.

## 4. Integrating along the saddle point contours

We use numerical quadrature for the integral (10), considering a contour through the saddle point $w_0$. The relation in (18) gives the description of the steepest descent path on which $\Im\phi(w)$ is constant. This path is optimal from the viewpoint of numerical instabilities because the integrand is free of oscillations on this contour.

Integrating with respect to $\tau$ we obtain

$$\mathrm{Ai}(z) = \frac{\mathrm{e}^{-\zeta}}{2\pi\mathrm{i}}\int_{-\infty}^{\infty}\mathrm{e}^{\psi_r(\sigma,\tau)}\left(\frac{\mathrm{d}\sigma}{\mathrm{d}\tau} + \mathrm{i}\right)\mathrm{d}\tau, \tag{20}$$

$$\mathrm{Ai}'(z) = -\frac{\mathrm{e}^{-\zeta}}{2\pi\mathrm{i}}\int_{-\infty}^{\infty}\mathrm{e}^{\psi_r(\sigma,\tau)}[u_0 + \sigma + \mathrm{i}(v_0 + \tau)]\left(\frac{\mathrm{d}\sigma}{\mathrm{d}\tau} + \mathrm{i}\right)\mathrm{d}\tau, \tag{21}$$

where $\zeta = 2z^{3/2}/3$ and $\psi_r$ is given by (15); the relation between $\sigma$ and $\tau$ is (see (18)):

$$\sigma = \frac{\tau(\tau + 3v_0)}{3\left[u_0 + \sqrt{(\tau^2 + 4v_0\tau + 3r)/3}\right]}, \quad -\infty < \tau < \infty. \tag{22}$$

From this relation we can obtain $d\sigma/d\tau$, but we can also use (16) to obtain

$$\frac{d\sigma}{d\tau} = -\frac{\partial\psi_i/\partial\tau}{\partial\psi_i/d\sigma} = \frac{\tau^2 - \sigma^2 - 2u_0\sigma + 2v_0\tau}{2(v_0\sigma + u_0\tau + \sigma\tau)}. \tag{23}$$

For $\sigma$ and $\tau$ satisfying (22) we know that $\psi_i(\sigma, \tau) = 0$. Notice, besides, that at the saddle point $\partial\psi_i/\partial\tau = \partial\psi_i/\partial\sigma = 0$ by the Cauchy–Riemann equations and then $d\sigma/d\tau$, as expressed in (23), is not suitable for numerical computation. However, it is a simple matter to avoid cancellations by first dividing both the numerator and the denominator by $\tau$. This is a general feature when applying the saddle point method for numerical computations: the resulting integrals must be expressed in coordinates relative to the saddle point both to extract the dominant contribution and to avoid cancellations in the Jacobian.

The relation in (23) between $\sigma$ and $\tau$ becomes non-smooth at $\theta = 2\pi/3$. As can be seen from the steepest descent path in figure 2, the quantity $d\sigma/d\tau$ becomes bi-valued at the saddle point $-w_0$. This aspect will have influence on the efficiency when using a quadrature rule of values of $\theta$ close to $2\pi/3$, because of singularities near the path of integration in (20) and (21).

These singularities follow from the zeros of the square root in (22). We find that the zeros are

$$\sigma_\pm = -2v_0 \pm i\sqrt{r}\sqrt{3 - 4\sin^2\frac{\theta}{2}}, \quad 0 \leqslant \theta \leqslant \frac{2\pi}{3}. \tag{24}$$

We see that the singularities indeed approach the real axis when $\theta \to 2\pi/3$.

## 5. Modifying the saddle point contours

For values of $\theta$ close to $2\pi/3$ we replace the steepest descent path defined in (18) by a path that

(1) remains smooth if $\theta \to 2\pi/3$;

(2) passes the saddle point $w_0$;

(3) the direction at the saddle point is as for the steepest descent contour, namely $(d\sigma/d\tau)_{\sigma=0,\tau=0} = \tan(\theta/4)$;

(4) runs into the valleys of $e^{\phi(w)}$ at $\mathrm{ph}w = \pm\pi/3$.

A simple choice of such a path is constructed by putting

$$u = \alpha + \beta v + \sqrt{\frac{1}{3}v^2 + \gamma}, \tag{25}$$

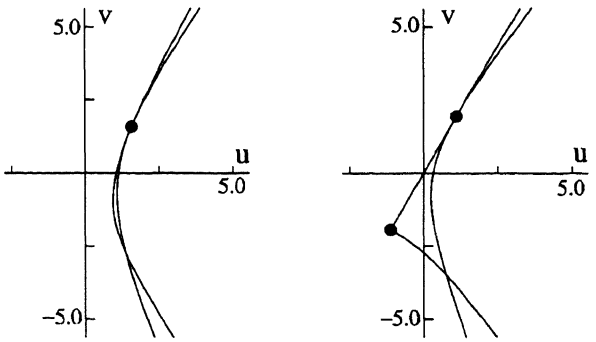


Figure 3. Steepest descent contours given by (18) and approximate contours based on (25) for $r = 5$ and $\theta = \pi/2$ (left) and $\theta = 2\pi/3$.

where $\alpha$, $\beta$, $\gamma$ are determined by the above four conditions. From (2) and (3) we obtain

$$u_0 = \alpha + \beta v_0 + \sqrt{\frac{1}{3}v_0^2 + \gamma}, \qquad \tan\frac{\theta}{4} = \beta + \frac{v_0}{3\sqrt{v_0^2/3 + \gamma}}.$$

To satisfy (4) we take $\beta$ small enough, and a convenient choice is

$$\beta = \frac{1}{3}\tan\frac{\theta}{4}.$$

This gives

$$\alpha = -\frac{5}{3}\sqrt{r}\sin^2\frac{\theta}{4}, \qquad \gamma = \frac{1}{3}r\cos^2\frac{\theta}{4}\left(3 - 7\sin^2\frac{\theta}{4}\right).$$

In figure 3 we draw exact steepest descent contours and approximate contours based on (25) for $r = 5$ and $\theta = \pi/2, \theta = 2\pi/3$.

For the modified contour the singularities occur when the square root in (25) is zero. We find

$$\sigma_{\pm}^{a} = -v_0 \pm \mathrm{i}\sqrt{r}\cos\frac{\theta}{4}\sqrt{3 - 7\sin^2\frac{\theta}{4}}. \tag{26}$$

and the imaginary part is now bounded away from zero when $|\mathrm{phz}| \leqslant 2\pi/3$.

In the numerical algorithm we use the modified contour defined in (25) for $\pi/2 < \theta \leqslant 2\pi/3$ and the exact steepest descent path for $0 \leqslant \theta \leqslant \pi/2$.

When $r$ tends to zero again singularities arise: the singularities in (24) and (26) approach the origin if $r \to 0$. These singularities are of no concern, because efficient methods of computation for small $r$ can be based on the Maclaurin expansions of the Airy function and its derivative.

In any case, we can define a contour for small values of $r$ by writing, for example,

$$u = u_0 + \sqrt{\frac{1}{3}v^2 + 1} - \sqrt{\frac{1}{3}v_0^2 + 1},$$

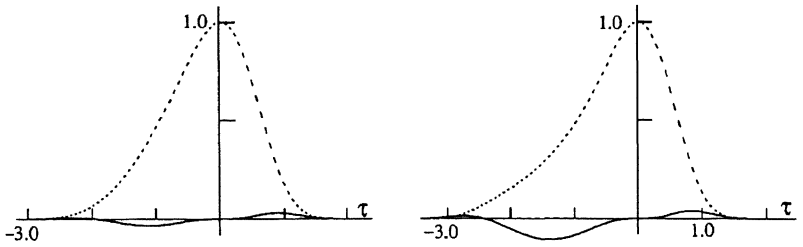


Figure 4. Graphs of $e^{\psi_r(\sigma,\tau)} \cos \psi_i(\sigma, \tau)$ (dashed) and $e^{\psi_r(\sigma,\tau)} \sin \psi_i(\sigma, \tau)$ for the modified contours, with $r = 1$ and $\theta = \pi/2$ (left) and $\theta = 2\pi/3$.

and use this as an alternative for $r \leqslant 1$. For these values no instabilities arise and the contributions from a neighborhood of the saddle point are less dominant. In this way we can use numerical quadrature for all complex values of $z$.

In figure 4 we show the graphs of $e^{\psi_r(\sigma,\tau)} \cos \psi_i(\sigma, \tau)$ and $e^{\psi_r(\sigma,\tau)} \sin \psi_i(\sigma, \tau)$ for the modified contours. Observe that now $\psi_i(\sigma, \tau)$ is not identically zero, as for the case of the exact steepest descent contour. For $r = 1$ we see little oscillations in $e^{\psi_r(\sigma,\tau)} \sin \psi_i(\sigma, \tau)$.

The trapezoidal rule is used to compute these integrals, being the accuracy of the computation determined by the step size and the truncation of the series approximating the integral. Given that the integrals considered all converge very fast at infinity ($\psi_r(\sigma, \tau) \sim -c|\tau|^3$ as $\tau \to \pm\infty$ with $c > 0$), convergence of the series is of no concern. Besides, given that the functions under the integration are analytic in a strip along the real axis and decaying exponentially at infinity, the error due to the step size is exponentially decreasing with decreasing $h$; see [9].

The method based on steepest descent contours and modified contours can be used to compute scaled complex Airy functions $e^{\zeta}\mathrm{Ai}$, $e^{\zeta}\mathrm{Ai}'$ to any desired accuracy. The accuracy of the trapezoidal rule for computing these integrals can be easily adjusted by modifying the step size.

## 6. Gauss–Laguerre quadrature

The method we now describe, based on Gauss quadrature, can be used for the fast computation of Airy functions to a predetermined accuracy. This method is to be used for a fixed precision, determined by the order of the Gauss quadrature.

The approach stems from the relation between Airy functions and modified Bessel functions:

$$\mathrm{Ai}(z) = \frac{1}{\pi}\sqrt{\frac{z}{3}}K_{1/3}(\zeta), \qquad \mathrm{Ai}'(z) = -\frac{z}{\pi\sqrt{3}}K_{2/3}(\zeta), \tag{27}$$

where $\zeta = 2z^{3/2}/3$, and the integral representation [1, equation (9.6.23)]

$$K_\nu(z) = \frac{\sqrt{\pi}}{2^\nu\Gamma(\nu + 1/2)}\frac{e^{-z}}{\sqrt{z}}\int_0^\infty \left(2 + \frac{t}{z}\right)^{\nu-1/2} t^{\nu-1/2}e^{-t}\,dt, \tag{28}$$

which can be adequately computed with the generalized Gauss–Laguerre quadrature rule. Gautschi [4] considered this integral representation for the computation of $\mathrm{Ai}(x)$ for real $x > 1$.

We have for $z \neq 0$, $|\mathrm{ph}\zeta| < \pi$:

$$\begin{aligned}
\mathrm{Ai}(z) &= a(z)\int_0^\infty \left(2+\frac{t}{\zeta}\right)^{-1/6} t^{-1/6}\mathrm{e}^{-t}\,\mathrm{d}t,\\
a(z) &= \frac{1}{\sqrt{\pi}(48)^{1/6}\Gamma(5/6)}\mathrm{e}^{-\zeta}\zeta^{-1/6},\\
\mathrm{Ai}'(z) &= b(z)\int_0^\infty \left(2+\frac{t}{\zeta}\right)^{1/6} t^{1/6}\mathrm{e}^{-t}\,\mathrm{d}t,\\
b(z) &= -\frac{z}{\sqrt{3\pi}2^{2/3}\Gamma(7/6)}\frac{\mathrm{e}^{-\zeta}}{\sqrt{\zeta}},
\end{aligned} \tag{29}$$

which can be computed by using Gauss–Laguerre quadrature with parameters $\alpha = -1/6$ and $\alpha = 1/6$, respectively, at least on the positive real axis and not too small $x$. According the Gautschi [4] a 36-point Gauss suffices to compute $\mathrm{Ai}(x)$, $x > 1$, to double precision accuracy. However, for computing Airy functions in the complex plane it turns out that 36 points is not enough. Instead, we will take 40 points.

An additional problem is the presence of singularities in the integrands in the complex plane. When extending the integrals to the complex plane the computation becomes unstable as $z$ approaches the boundary of the principal sector $\mathcal{S}$, that is the the Stokes line at $\theta = 2\pi/3$. The reason is the presence of singularities in the integrand at $t = -2\zeta$, which become real as $\theta \to 2\pi/3$. This problem can be circumvented by turning the path of integration over a given angle $\tau$. This can be done by the substitution $t \to t(1+\mathrm{i}\tan\tau)$ in (29), and we arrive at

$$\begin{aligned}
\mathrm{Ai}(z) &= a(z)\left(\frac{\mathrm{e}^{\mathrm{i}\tau}}{\cos\tau}\right)^{5/6}\int_0^\infty \left(2+\frac{t}{\widetilde{\zeta}}\right)^{-1/6} \mathrm{e}^{-\mathrm{i}t\tan(\tau)}t^{-1/6}\mathrm{e}^{-t}\,\mathrm{d}t,\\
\mathrm{Ai}'(z) &= b(z)\left(\frac{\mathrm{e}^{\mathrm{i}\tau}}{\cos\tau}\right)^{7/6}\int_0^\infty \left(2+\frac{t}{\widetilde{\zeta}}\right)^{1/6} \mathrm{e}^{-\mathrm{i}t\tan(\tau)}t^{1/6}\mathrm{e}^{-t}\,\mathrm{d}t,
\end{aligned} \tag{30}$$

where $\widetilde{\zeta} = \cos\tau\mathrm{e}^{-\mathrm{i}\tau}\zeta$. A convenient choice of $\tau$ is $\tau = 3(\theta - \pi/2)/2$. At $\theta = \pi/2$ the expressions (29) and (30) coincide and for $\pi/2 < \theta \leqslant 2\pi/3$ the new integrands are free of singularities.

As a result, we can safely use the integrals (29) for $0 \leqslant \theta \leqslant \pi/2$ and these in (30) for $\pi/2 < \theta \leqslant 2\pi/3$, both cases for not too small $|z|$. Of course, as $z$ becomes large the singularities have less influence, and the Gauss–Laguerre quadrature (with parameters $\alpha = \pm 1/6$) tends to work better. In any case, small values of $|z|$ are of no concern, because then the Airy functions can be accurately computed from power series.

## 7. Numerical verification of the algorithms

The method based on steepest descent paths and modified paths described in sections 3, 4 and 5, being of adjustable accuracy, can be used as a test-bench in order to set the parameters of Gauss–Laguerre integration (section 6), namely, how many Gauss points should be considered, how many of these points are relevant for the computation to a given accuracy and where are the regions where alternative methods should be considered.

The use of power series for small $|z|$ should be considered as complement to the Gauss–Laguerre quadrature. The number of required Gauss points tends to increase with decreasing $|z|$; therefore, using series for small $|z|$ gives us the chance of using less Gauss points in the rest of the complex plane; a compromise has to be found between the number of Gauss points and the rate of convergence of series. On the other hand, when $|z|$ becomes large, asymptotic expansions [1, equation (10.4.59)] will be faster than any other method. Simple error bounds are available for the remainders (see [10, pp. 394, 269]).

We test the accuracy of the modulus and phase of Airy functions for these different methods of computation, both for scaled ($e^{\zeta}\,\mathrm{Ai}$, $e^{\zeta}\,\mathrm{Ai}'$) and unscaled functions. In order to reduce overflow problems, we check the accuracy in the computation of $\mathrm{Mo}(z) \equiv |\Re(A_i(z))| + |\Im(A_i(z))|$ and of $\mathrm{Ra}(z) \equiv \min(\Re(A_i(z))/\Im(A_i(z)), \Im(A_i(z))/\Re(A_i(z)))$ (and similarly for the derivative and the scaled functions). We should demand that $\mathrm{Mo}(z)$ maintains its accuracy throughout the complex plane except in the close vicinity of the zeros of $\mathrm{Ai}(z)$, where relative errors loose their meaning; as for $\mathrm{Ra}(z)$, we can expect that some accuracy is lost near the level curves $\Re(\mathrm{Ai}) = 0$ and $\Im(\mathrm{Ai}) = 0$.

We next explore the regions of application of series, Gauss quadrature and asymptotic expansions for building an algorithm aimed at a precision of $10^{-13}$. In order to perform these tests, it is more convenient to consider scaled Airy functions rather than unscaled ones. The reason for this is twofold: first, the scaled Airy functions do not overflow/underflow for large $|z|$; second, it is easier to achieve higher accuracy when evaluating scaled functions, given that the factor $\exp(\zeta)$ (with $\zeta = 2z^{3/2}/3$) is not needed. This factor introduces loss of precision, as can be easily understood given that

$$e^{\zeta} = \exp(r_0 \cos\phi)\big[\cos(r_0 \sin\phi) + \mathrm{i}\sin(r_0 \sin\phi)\big]$$

with $r_0 = 2|z|^{3/2}/3$ and $\phi = 2\mathrm{ph}z/3$. Then, as $r_0$ becomes large the arguments are large and will cause severe absolute errors in the values of $\cos(r_0 \sin\phi)$ and $\sin(r_0 \sin\phi)$, and large relative errors in $\exp(r_0 \cos\phi)$. This type of loss of precision in these elementary functions can be expected both in the modulus and in the phase.

It is important to note that the scaled functions $\widetilde{\mathrm{Ai}}(z) = e^{\zeta}\mathrm{Ai}(z)$ and $\widetilde{\mathrm{Ai}}'(z) = e^{\zeta}\mathrm{Ai}'(z)$ present a discontinuity cut at $\Re z < 0$, and consequently, the connection formulas (5) for $2\pi/3 < \mathrm{ph}z \leqslant \pi$ must be substituted by

$$\widetilde{\mathrm{Ai}}(z) = -e^{-2\pi\mathrm{i}/3}e^{4z^{3/2}/3}\widetilde{\mathrm{Ai}}\big(ze^{-2\pi\mathrm{i}/3}\big) - e^{2\pi\mathrm{i}/3}\widetilde{\mathrm{Ai}}\big(ze^{2\pi\mathrm{i}/3}\big) \tag{31}$$

and similarly for the derivative.

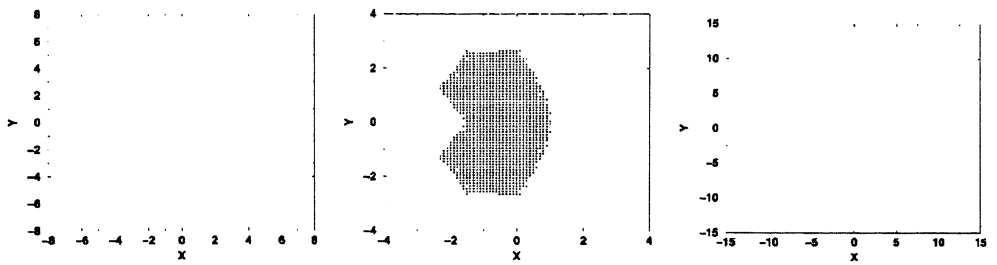


Figure 5. Points where Maclaurin series (a), Gauss–Laguerre method (b) and asymptotic expansions (c) fail to produce results with an accuracy of $10^{-13}$. These methods are compared with the stable saddle point integral representations, using as test function $|\Re(\widetilde{\mathrm{Ai}})|+|\Im(\widetilde{\mathrm{Ai}})|$ (the comparison for $|\Im(\widetilde{\mathrm{Ai}})|/|\Re(\widetilde{\mathrm{Ai}})|$ yields similar results).

Let us first check the possible range of application of Maclaurin series for $\widetilde{\mathrm{Ai}}(z)$ and $\widetilde{\mathrm{Ai}}'(z)$ [1, equation (10.4.2)] by comparing them with the saddle point methods here described. We see (figure 5(a)) that loss of precision takes place for $x > 2$ and then we should consider Gauss–Laguerre quadrature for such values. This fact sets limits on the number of Gauss points that are needed. Notice that for $\Re(z) < 0$ the region where series are accurate is considerably wider. However, as $|z|$ increases more terms are needed and quadrature will be more efficient.

A 40-point Gauss–Laguerre quadrature is sufficient to cover the region where series fail. Of these 40 points only the first 25 are relevant and we can drop the rest. The resulting $10^{-13}$-precision test, by comparing with saddle point integrals, is shown in figure 5(b). We observe that the region where the Gauss–Laguerre method is inaccurate is safely covered by Maclaurin series.

Finally, when asymptotic expansions [1, equation (10.4.59)] succeed in producing accurate values, we should use them. Figure 5(c) shows the region where asymptotic series fail to produce results with a precision of $10^{-13}$.

All these results apply equally for $\widetilde{\mathrm{Ai}}(z)$ and $\widetilde{\mathrm{Ai}}'(z)$.

An algorithm to efficiently compute complex Airy functions to a fixed precision (better than $10^{-13}$) could, therefore, be based on:

1. Maclaurin series for moderate $|z|$; for instance: $-3 \leqslant x \leqslant 1.5$, $-3 \leqslant y \leqslant 3$ $(z = x + \mathrm{i}y)$.
2. Asymptotic expansions for large $|z|$ ($|z| \geqslant 15$ is a sound choice).
3. Gauss–Laguerre quadrature for intermediate values of $|z|$; we recommend 40-point Gauss–Laguerre quadrature outside the power series region with $|z| < 15$.

With this we can build a fast code for a fixed precision of $10^{-13}$ for the computation of scaled Airy functions. For unscaled Airy functions, as commented before, it is much more difficult to attain a uniform accuracy in all the complex plane and some loss of accuracy is expected as $|z|$ increases, as shown in figure 6. In figure 6 we show the

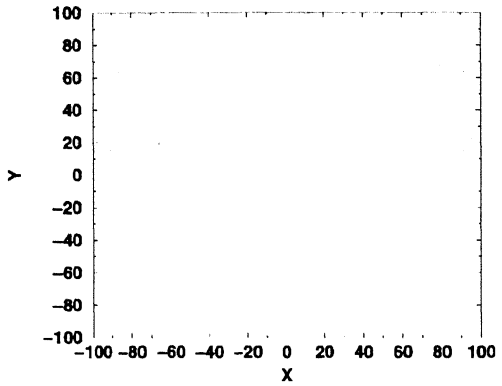


Figure 6. Comparison between the combined methods (series, Gaussian integration and asymptotic expansions) and the saddle point integrals. The function $|\Re(\mathrm{Ai})|+|\Im(\mathrm{Ai})|$ is tested for an accuracy of $10^{-13}$. The points of discrepancy between both approaches are found. In the darker shaded regions the Airy function overflows.

comparison between the combined algorithm and the saddle point integrals. Some loss of precision takes place as $|z|$ increases and none of the methods is responsible for these inaccuracies; as before discussed, the dominant contribution $e^{-\zeta}$ is the source of errors.

### *7.1. Comparison with Amos' code*

We have also tested the quadrature methods against the code developed by Amos [2], which also has the option of computing scaled Airy function. This algorithm is based on the evaluation of complex modified Bessel functions (27). The principal sector for the computation of the modified Bessel functions in Amos' code is $\Re(\zeta) > 0$, while for $\Re(\zeta) < 0$ continuation formulas involving the $K$ and $I$ Bessel functions are considered [1, equation (9.6.30)].

These tests show that our Gauss–Laguerre method is generally faster and that it is more accurate near the anti-Stokes lines and close to the positive real axis when $1 < z < 2$. In these regions Amos' code fails to provide $10^{-13}$ precision. We observe these discrepancies both when comparing with the saddle point integrals and the combined algorithm with Gauss–Laguerre quadrature, while there is perfect match ($10^{-13}$ precision) between both quadrature algorithms. Discrepancies persist for an accuracy of $10^{-12}$, particularly near the anti-Stokes lines.

More details will be given in a forthcoming paper [6].

## Acknowledgements

A. Gil acknowledges support from A. von Humboldt Foundation. J. Segura acknowledges support from DAAD.

## References


[1] M. Abramowitz and I.A. Stegun (eds.), *Handbook of Mathematical Functions*, National Bureau of Standards Applied Mathematics Series No. 55 (US Government Printing Office, Washington, DC, 1964).

[2] D.E. Amos, Algorithm 644: A portable package for Bessel functions of a complex argument and nonnegative order, ACM Trans. Math. Softw. 12 (1986) 265–273.

[3] R.M. Corless, D.J. Jeffrey and H. Rasmussen, Numerical evaluation of Airy functions with complex arguments, J. Comput. Phys. 99 (1992) 106–114.

[4] W. Gautschi, Computation of Bessel and Airy functions and of related Gaussian quadrature, BIT 42 (2002) 110–118.

[5] A. Gil, J. Segura and N.M. Temme, On non-oscillating integrals for computing inhomogeneous Airy functions, Math. Comput. 70 (2001) 1183–1194.

[6] A. Gil, J. Segura and N.M. Temme, AiZ: a Fortran program for the computation of complex Airy functions (submitted).

[7] E.T. Goodwin, The evaluation of integrals of the form $\int_{-\infty}^{\infty} f(x)\mathrm{e}^{-x^2}\,\mathrm{d}x$, Cambridge Phil. Soc. Proc. 45 (1949) 241–245.

[8] D.W. Lozier and F.W.J. Olver, Numerical evaluation of special functions, in: *AMS Proceedings of Symposia in Applied Mathematics*, Vol. 48, ed. W. Gautschi (1994) pp. 79–125.

[9] Y.L. Luke, *The Special Functions and Their Approximations*, Vol. I–II (Academic Press, New York, 1969).

[10] F.W.J. Olver, *Asymptotics and Special Functions* (Academic Press, New York, 1974, reprinted by A.K. Peters, 1997).

[11] Z. Schulten, D.G.M. Anderson and R.G. Gordon, An algorithm for the evaluation of complex Airy functions, J. Comput. Phys. 31 (1979) 60–75.

[12] N.M. Temme, *Special Functions: An Introduction to the Classical Functions of Mathematical Physics* (Wiley, New York, 1996).

[13] R. Wong, *Asymptotic Approximations of Integrals* (Academic Press, New York, 1989).